

A Six Vertex Model on a Fishnet

Charles B. Thorn*

*Institute for Fundamental Theory
Department of Physics, University of Florida, Gainesville, FL 32611*

Abstract

The flow of $U(1)$ charge through dense fishnet diagrams, in a non-hermitian matrix scalar field theory $g_1 \text{Tr}(\Sigma^\dagger \Sigma)^2 + 2g_1 v \text{Tr} \Sigma^{\dagger 2} \Sigma^2$, is described by a 6-vertex model on a “diamond” lattice [1]. We give a direct calculation of the continuum properties of the 6-vertex model on this novel lattice, explicitly confirming the conclusions of [1], that, for $1/2 \leq v < \infty$, they are identical to those of a world-sheet scalar field compactified on a circle S_1 . The radius of the circle is related to the ratio v of quartic couplings by $R^{-2} = 2T_0 \cos^{-1}(1 - 1/2v^2)$. This direct computational approach may be of value in generalizing the conclusions to the non-Abelian $O(n)$ case.

*E-mail address: thorn@phys.ufl.edu

1 Introduction

We are accustomed in string and related theories to the apparent need for more than four space-time dimensions. On the other hand, the conjectured equivalence (duality), between some ordinary four dimensional supersymmetric quantum field theories and string theories on certain ten dimensional space-time manifolds [2], suggests that these extra dimensions may be but a mathematical device that conveniently reflects some other aspect of the underlying theory.

In the late 1970's, we showed how a single extra compact dimension effectively arises in the context of the fishnet diagram model of a string world-sheet in a scalar quantum field theory with an $O(2) \equiv U(1)$ global symmetry [1]. It is plausible that in field theories with a richer symmetry, for instance $SO(n)$, multiple compact dimensions (perhaps S_{n-1}) will arise from the same mechanism.

As an important preliminary to extending the work of [1] to higher symmetries, we give in this article a new derivation of the main results of [1] that doesn't rely on indirect arguments, such as invoking $\sigma \leftrightarrow \tau$ symmetry (modular invariance) and the universality of the continuum limit. Instead, we obtain all the results by direct and explicit computation. The methods used here are fairly standard, borrowed from the mathematical analysis of one-dimensional Heisenberg spin chains by Yang and Yang [3] and from that of the 6-vertex models by Lieb [4] and others [5]. However our particular model involves several novel details, e.g. a non-standard lattice, not present in those classic treatments, and we think our direct approach illuminates these features in a useful way.

The fishnet model [6] as formulated in [7] is obtained in the context of a discretized light-cone parameterization of the propagators of an $N_c \times N_c$ matrix quantum field theory:

$$D(\mathbf{p}, p^+, x^+) = \theta(\tau) \frac{1}{2p^+} e^{-\tau \mathbf{p}^2 / 2p^+} \rightarrow \frac{1}{2l} e^{-k \mathbf{p}^2 / 2lT_0} \quad (1)$$

where $p^+ = lm$ and $\tau \equiv ix^+ = ka \equiv km/T_0$ with k, l running over all positive integers. Planar diagrams are singled out by 't Hooft's $N_c \rightarrow \infty$ limit. All propagators of the fishnet diagrams (see Fig. 1) of [7] are restricted to $k = l = 1$. For a fixed total $P^+ = Mm$ and fixed evolution time

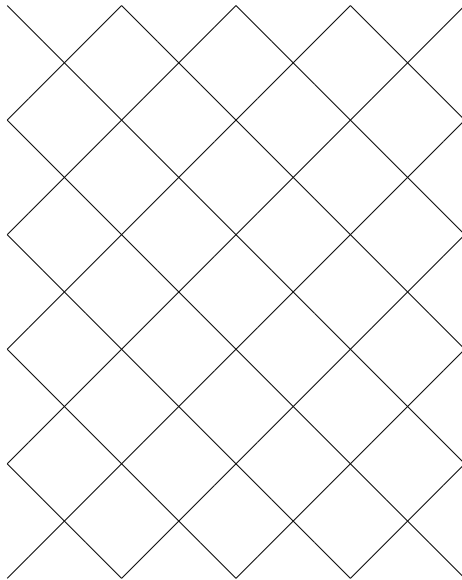


Figure 1: Fishnet diagram for a scalar quantum field theory with only quartic interactions.

$T = Na$, this restriction achieves the maximal density of vertices, and is plausibly appropriate for strong coupling. In [1] and also here, the focus is on how to deal with internal degrees of freedom carried by the propagators of these fishnet diagrams. We simply accept the simplest fishnet *ansatz* as a working model for string formation. As discussed in [8] there is a lot of room for improvements in the fishnet model itself, but we don't consider those issues here.

Thus the sum of fishnet diagrams provides a model of the discretized world-sheet [9] of light-cone string theory [10]. The main piece of physics we draw from the model is that M and N , which determine the size and shape of the lattice world-sheet, are determined by the P^+ , carried by the system of field quanta propagated by the diagram, and by the time span over which that system evolves. In the continuum limit $N/M \rightarrow T/P^+T_0$, so that energy (P^-) eigenvalues E_r can be read off from the exponential dependence on N of the sum over diagrams $\sim e^{-NaE_r}$.

Notice that the fishnet diagram determines a novel two dimensional square lattice in which all links are rotated by 45 degrees. We refer to such a lattice as a diamond lattice. One of the lacunae in [1] was the reliance on known results for a conventional square lattice plus the reasonable assertion that the continuum limit should be isotropic. Our calculation here deals directly with the diamond lattice configuration, and the details of the computation are therefore new. In particular we develop an appropriate adaptation of the Bethe *ansatz* [11] to the diamond lattice.

2 The Model

The field theory analyzed in [1] is the special case $n = 2$ of a matrix scalar field Σ_i transforming as a vector under $O(n)$ with quartic interaction terms that respect this symmetry:

$$\mathcal{L} = -\frac{1}{2}\text{Tr}(\partial\Sigma_i)^2 - \frac{\mu^2}{2}\text{Tr}\Sigma_i^2 - \frac{g_1}{2}\text{Tr}\Sigma_i^2\Sigma_j^2 - \frac{g_2}{4}\text{Tr}\Sigma_i\Sigma_j\Sigma_i\Sigma_j. \quad (2)$$

For $n = 2$ it is convenient to define a single non-hermitian matrix field $\Sigma \equiv (\Sigma_1 + i\Sigma_2)/\sqrt{2}$ which carries a unit $U(1) \equiv SO(2)$ charge. The interaction terms then become

$$V(\Sigma) = (g_1 + g_2)\text{Tr}\Sigma^{\dagger 2}\Sigma^2 + g_1\text{Tr}\Sigma^{\dagger}\Sigma\Sigma^{\dagger}\Sigma. \quad (3)$$

The charge carried by a given line in a diagram is indicated by attaching an arrow pointing in the direction of charge flow. There are precisely six (planar) charge conserving vertices (see Fig. 2): Two

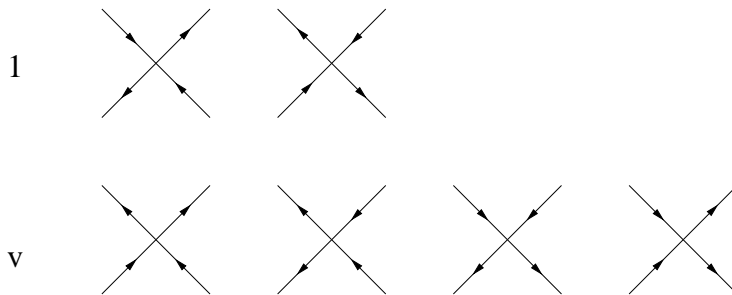


Figure 2: $U(1)$ Vertices: $v = (g_1 + g_2)/2g_1$

with weight $2g_1$ in which each adjacent pair carries charge 0 into the vertex, and four with weight $g_1 + g_2 \equiv 2vg_1$ in which two adjacent lines carry charge 2 into the vertex. Scaling $g_1, g_2 \rightarrow \lambda g_1, \lambda g_2$ just multiplies the diagram by an overall factor λ^{MN} , so we lose nothing by scaling $2g_1$ to 1, so

the weights of the two classes of vertices are $1, v$ respectively. A typical fishnet diagram with these vertices is shown in Fig. 3. The sum of all such diagrams is thus seen to be equivalent to calculating the partition function for a 6-vertex model on a diamond lattice.

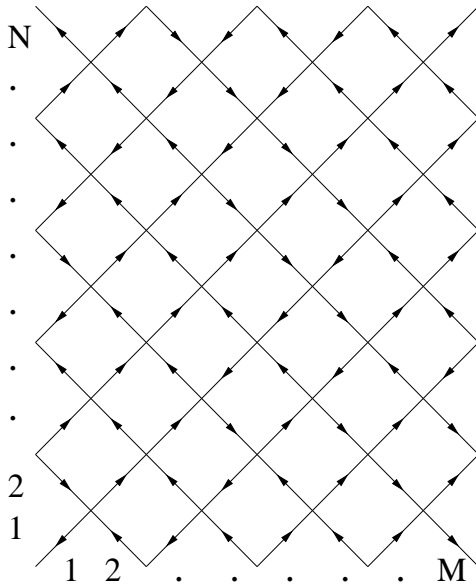


Figure 3: Fishnet propagating M units of P^+ N steps in time. Periodic boundary conditions have been imposed.

3 The transfer Matrix and its Eigenvalues

The fishnet diagram can be thought of as a discrete (imaginary) time evolution of a state which is a tensor product of M two state systems, (“spins”), labeled by up and down arrows. Because of the diamond lattice configuration, the basic discrete evolution is two time steps, and we define each element of the $2^M \times 2^M$ transfer matrix \mathcal{T} as the product of vertex factors associated with the subgraph that connects a given row of arrows with the row two time steps above it. It is easy to see that the state with all arrows up or all arrows down is an eigenstate of the transfer matrix with eigenvalue v^M .

3.1 One overturned arrow: $Q = M - 2$

Let us next consider the states with one overturned arrow, i.e. $M - 1$ up arrows and 1 down arrow. With periodic boundary conditions, even and odd locations for this down arrow are not equivalent, because of the diamond lattice. Denote the state with down arrow at location j by $|j\rangle$. Then, by following the change in j after two time steps we find the action of the transfer matrix

$$\mathcal{T}|j\rangle = \begin{cases} |j+2\rangle v^M + |j+1\rangle v^{M-1} + |j-1\rangle v^{M-1} + |j\rangle v^{M-2} & \text{for } j \text{ odd} \\ |j-2\rangle v^M + |j+1\rangle v^{M-1} + |j-1\rangle v^{M-1} + |j\rangle v^{M-2} & \text{for } j \text{ even.} \end{cases} \quad (4)$$

Note, by the way, that the action of \mathcal{T} is local in that the down spin migrates at most two sites after two time steps.[†] Thus, in representing a spin wave as a Fourier transform with respect to

[†]In contrast, for the 6-vertex model on a conventional square lattice, the down spin can be on any site after a single time step. This is one sense in which the diamond lattice is superior from a physical point of view.

location, we must allow for a phase shift in the even terms with respect to the odd terms:

$$|k\rangle = \sum_{j \text{ odd}} |j\rangle e^{ikj} + \xi(k) \sum_{j \text{ even}} |j\rangle e^{ikj} \quad (5)$$

Applying the transfer matrix to the state $|k\rangle$ and shifting the sums over j appropriately, we find that $|j\rangle e^{ikj}$ is multiplied by the factor

$$\begin{aligned} v^{M-2} + e^{-2ik} v^M + \xi(k) e^{ik} v^{M-1} + \xi(k) e^{-ik} v^{M-1} & \quad \text{for } j \text{ odd} \\ \xi(k) v^{M-2} + \xi(k) e^{2ik} v^M + e^{ik} v^{M-1} + e^{-ik} v^{M-1} & \quad \text{for } j \text{ even,} \end{aligned} \quad (6)$$

for $j \neq 1, M$. For $|k\rangle$ to be an eigenstate of \mathcal{T} , these two factors must agree, which determines a quadratic equation for $\xi(k)$:

$$\xi^2 - (2iv \sin k)\xi - 1 = 0. \quad (7)$$

It is easy to see that interchanging the two solutions for ξ interchanges the eigenstate $|k\rangle$ with $-|k + \pi\rangle$. Thus we lose no generality in selecting the solution

$$\xi(k) \equiv iv \sin k + \sqrt{1 - v^2 \sin^2 k} \quad (8)$$

provided we allow k the full 2π range, $-\pi < k \leq \pi$. (Keeping both solutions would require restricting the range of k to π to avoid double counting.) When the transfer matrix acts on arrows near $j = 1, M$, it wraps around with the location 1 equivalent to $M + 1$, M equivalent to 0, etc. These terms must match for $|k\rangle$ to be an eigenstate, which requires $e^{iMk} = 1$ or

$$k = \frac{2\pi n}{M} \quad \text{for } n = 0, 1, 2, \dots, M-1. \quad (9)$$

Putting the selected solution for $\xi(k)$ back into one of the factors (6), we find the eigenvalue of the transfer matrix to be $v^M t(k)$ where

$$t(k) = \left(\cos k + \frac{1}{v} \sqrt{1 - v^2 \sin^2 k} \right)^2. \quad (10)$$

It is a welcome outcome that the eigenvalue is automatically positive as long as $v^2 \sin^2 k < 1$.

3.2 Two or more overturned arrows: $Q = M - 2q$

Moving on to two overturned arrows, we employ the Bethe *ansatz* for two overturned arrows appropriate to our diamond lattice:

$$\begin{aligned} |k_1, k_2\rangle = & \left[\sum_{l \text{ odd}} \sum_{m \text{ odd}} +\xi_1 \sum_{l \text{ even}} \sum_{m \text{ odd}} +\xi_2 \sum_{l \text{ odd}} \sum_{m \text{ even}} +\xi_1 \xi_2 \sum_{l \text{ even}} \sum_{m \text{ even}} \right] |l, m\rangle e^{ilk_1 + imk_2} \\ & + A(1, 2) (k_1, \xi_1 \leftrightarrow k_2, \xi_2) \end{aligned} \quad (11)$$

For q overturned arrows, the Bethe *ansatz* is the obvious generalization, wherein the sum over $1 \leftrightarrow 2$ is replaced by a sum over all permutations of the spins, and $A(1, 2)$ is generalized to an A_P for each permutation. A_P factors into a product of $A(k, l)$ for each pair interchange needed to accomplish

the permutation. When the Bethe *ansatz* succeeds, as it does for this model, the eigenvalue of the transfer matrix is just

$$T(k_1, \dots, k_q) = v^M \prod_{j=1}^q t(k_j). \quad (12)$$

By explicitly analyzing the case $q = 2$, we find after much tedious algebra that

$$A(1, 2) = -\frac{(1 - 1/v^2)z_2 - z_1 - z_1 z_2/v - 1/v}{(1 - 1/v^2)z_1 - z_2 - z_1 z_2/v - 1/v}, \quad (13)$$

where we have defined $z_j \equiv \xi(k_j)e^{ik_j}$. Finally, the conditions that the periodic boundary conditions are consistent with the *ansatz* being an eigenstate are

$$e^{iMk_2} = A(1, 2), \quad e^{iMk_1} = A(2, 1) = 1/A(1, 2). \quad (14)$$

Since the permutation factor A_P for q overturned arrows is built up from pair factors, the $q = 2$ case is sufficient to determine all of the information we need to handle the general case, which leads to the boundary conditions

$$e^{iMk_l} = \prod_{j \neq l} A(j, l). \quad (15)$$

4 Analysis of the continuum limit: $M, N \rightarrow \infty$

For analyzing these equations it is convenient [3] to map the k_j onto new variables α_j for which $A(j, l)$ depends only on the difference $\alpha_j - \alpha_l$. This is accomplished by the map

$$\begin{aligned} z &= \xi e^{ik} = \frac{e^{i\nu} - e^\alpha}{e^{i\nu+\alpha} - 1} \\ e^{i\nu} &= \frac{1}{2v} + i\sqrt{1 - \frac{1}{4v^2}}. \end{aligned} \quad (16)$$

Note that our parameter ν is related to a similar parameter μ in [3] by $\mu = 2\nu$, which we shall also occasionally use. This version of the map is appropriate for $\infty > v \geq 1/2$, for which $e^{i\nu}$ is a pure phase. The case $v < 1/2$ must be handled separately. Some special values of α delineate the map: $\alpha = 0$ corresponds to $e^{ik}\xi = 1$ which implies $k = 0$, and $\alpha = \pm\infty$ map to $k = \pm(\pi - 2\nu)$. (We are choosing k to be in the range $-\pi < k < \pi$.) Thus the whole range $-\infty < \alpha < \infty$ corresponds to $-(\pi - 2\nu) < k < \pi - 2\nu$. Note that $v \rightarrow \infty$ shrinks the range of k to 0, whereas $v \rightarrow 1/2$ represents the maximum range. It is straightforward to work out the following quantities in terms of the new variables:

$$\begin{aligned} \tan k &= \frac{\sin 2\nu \sinh \alpha}{\cos \nu - \cos 2\nu \cosh \alpha} \\ \frac{dk}{d\alpha} &= \frac{\sin 3\nu}{2[\cosh \alpha - \cos 3\nu]} + \frac{\sin \nu}{2[\cosh \alpha - \cos \nu]} \\ t(k) &= \left(\cos k + \frac{1}{v} \sqrt{1 - v^2 \sin^2 k} \right)^2 = \frac{\cosh \alpha - \cos 3\nu}{\cosh \alpha - \cos \nu} \\ A &= -\frac{1 - e^{\beta-\alpha-4i\nu}}{e^{\beta-\alpha} - e^{-4i\nu}} \equiv -e^{i\theta(\alpha, \beta)} \\ \theta(\alpha, \beta) &= 2 \tan^{-1} \cot 2\nu \tanh((\beta - \alpha)/2) \end{aligned} \quad (17)$$

Using the last two equations, we can express the boundary conditions in the alternative forms

$$\begin{aligned} e^{iMk_l} &= \prod_{j \neq l} A(j, l) = (-)^{q-1} e^{i \sum_{j \neq l} \theta(\alpha_j, \alpha_l)} \\ k_l &= \frac{2\pi I_l}{M} + \frac{1}{M} \sum_{j \neq l} \theta(\alpha_j, \alpha_l), \end{aligned} \quad (18)$$

where the I_l are integers when q is odd, and they are half-odd integers when q is even. Different choices for these integers lead to different solutions for the set of k 's. Yang and Yang [3] encounter similar equations in their analysis of the x, y Heisenberg spin chain, and their techniques for solving them in the limit $M \rightarrow \infty$ can be directly applied. For easy comparison, we attempt as far as possible to adopt their notation.

4.1 Consecutive I_l : $Q, P \neq 0$

We begin by first choosing the set of numbers I_l to be consecutive with no gaps: $I_{l+1} = 1 + I_l$. We define a kernel K and density function $R(\alpha)$ by

$$\begin{aligned} K(\alpha, \beta) &\equiv \frac{1}{2\pi} \frac{\partial \theta}{\partial \beta} = \frac{1}{2\pi} \frac{\sin 4\nu}{\cosh(\alpha - \beta) - \cos 4\nu} \\ R(\alpha) &= \frac{2\pi}{M} \frac{dj}{d\alpha}, \end{aligned} \quad (19)$$

and then convert the equation for the k 's as $M \rightarrow \infty$ into an integral equation

$$\frac{dk}{d\alpha} = R(\alpha) + \int_{\alpha_-}^{\alpha_+} d\beta K(\alpha - \beta) R(\beta). \quad (20)$$

This equation has the same kernel K as the one analyzed in [3], but a different inhomogeneous term $dk/d\alpha$. The values chosen for α_{\pm} determine the characteristics of the eigenstate. For example, the eigenstate with maximum eigenvalue T for the transfer matrix corresponds to $\alpha_{\pm} = \pm\infty$. The values of k at the limits of this range are $k = \pm(\pi - 2\nu)$ and clearly $t(k) = 1$ for these values. As long as $0 < \nu < \pi/2$, $t(k) > 1$ for all finite α , so taking the whole range of α corresponds to including in the expression for T all values for t greater than unity. For the continuum limit we are only interested in very large α_{\pm} since then the eigenvalues will be close (within $1/M$) of the maximum eigenvalue.

As shown in [3], the kernel $J = -(I + K)^{-1}K$, can be used to rewrite the equation for R , which determines it over the whole range of α , in terms of its values outside the range (α_-, α_+) . This is useful since we are interested only in the excited states close to the ground state corresponding to $\alpha_{\pm} = \pm\infty$.

$$R(\alpha) = R_0(\alpha) - \left[\int_{-\infty}^{\alpha_-} + \int_{\alpha_+}^{\infty} \right] J(\alpha - \beta) R(\beta) \quad (21)$$

where R_0 is the solution of the equation for $\alpha_{\pm} = \pm\infty$. It can be easily found by Fourier transformation of the equation. From

$$\begin{aligned} \frac{dk}{d\alpha} &= \int d\lambda e^{-i\lambda\alpha} \frac{\sinh(\pi - 2\nu)\lambda \cosh \nu\lambda}{\sinh \pi\lambda} \\ K(\alpha) &= \int_{-\infty}^{\infty} \frac{d\lambda}{2\pi} e^{-i\lambda\alpha} \frac{\sinh(\pi - 2\nu)\lambda}{\sinh \pi\lambda}, \end{aligned} \quad (22)$$

we determine

$$\begin{aligned} R_0(\alpha) &= \int_{-\infty}^{\infty} d\lambda e^{-i\lambda\alpha} \frac{\cosh \nu\lambda}{2 \cosh 2\nu\lambda} \\ &= \frac{\pi}{\mu\sqrt{2}} \frac{\cosh(\pi\alpha/2\mu)}{\cosh(\pi\alpha/\mu)}. \end{aligned} \quad (23)$$

Recall that $\mu = 2\nu$.

We can also easily express J as a Fourier integral:

$$J(\alpha) = - \int_{-\infty}^{\infty} \frac{d\lambda}{2\pi} e^{-i\lambda\alpha} \frac{\sinh(\pi - 2\mu)\lambda}{2 \sinh(\pi - \mu)\lambda \cosh \mu\lambda}. \quad (24)$$

The conserved quantities $Q = M - 2q$, $P = \sum_j k_j$, the total charge and total momentum respectively can be expressed, in the limit $M \rightarrow \infty$, as integrals either inside or outside the range (α_-, α_+) . These expressions then implicitly determine α_{\pm} in terms of Q, P .

$$\begin{aligned} \frac{1}{2} - \frac{Q}{2M} = \frac{q}{M} &= \int_{\alpha_-}^{\alpha_+} \frac{d\beta}{2\pi} R(\beta) \\ &= \int_{-\infty}^{\infty} \frac{d\beta}{2\pi} R(\beta) - \left[\int_{-\infty}^{\alpha_-} + \int_{\alpha_+}^{\infty} \right] \frac{d\beta}{2\pi} R(\beta) \\ &= \frac{1}{2} - \left[\int_{-\infty}^{\alpha_-} + \int_{\alpha_+}^{\infty} \right] \frac{d\beta}{2\pi} R(\beta) \left(1 + \int_{-\infty}^{\infty} d\alpha J(\alpha - \beta) \right) \end{aligned} \quad (25)$$

Now,

$$1 + \int_{-\infty}^{\infty} d\alpha J(\alpha - \beta) = 1 - \frac{\pi - 2\mu}{2(\pi - \mu)} = \frac{\pi}{2(\pi - \mu)}, \quad (26)$$

so we have

$$\frac{Q}{M} = \frac{\pi}{\pi - \mu} \left[\int_{-\infty}^{\alpha_-} + \int_{\alpha_+}^{\infty} \right] \frac{d\beta}{2\pi} R(\beta). \quad (27)$$

In a similar manner we can express the total momentum as

$$\begin{aligned} \frac{P}{M} = \frac{1}{M} \sum_{j=1}^q k_j &= \int_{\alpha_-}^{\alpha_+} \frac{d\beta}{2\pi} R(\beta) k(\beta) \\ &= \int_{-\infty}^{\infty} \frac{d\beta}{2\pi} R(\beta) k(\beta) - \left[\int_{-\infty}^{\alpha_-} + \int_{\alpha_+}^{\infty} \right] \frac{d\beta}{2\pi} R(\beta) k(\beta) \\ &= \frac{P_0}{M} - \left[\int_{-\infty}^{\alpha_-} + \int_{\alpha_+}^{\infty} \right] \frac{d\beta}{2\pi} R(\beta) \left(k(\beta) + \int_{-\infty}^{\infty} d\alpha J(\alpha - \beta) k(\alpha) \right) \end{aligned} \quad (28)$$

We can infer the Fourier transform of $k(\alpha)$ from that of $dk/d\alpha$.

$$\begin{aligned} \frac{dk}{d\alpha} &= \int d\lambda e^{-i\lambda\alpha} \frac{\sinh(\pi - 2\nu)\lambda \cosh \nu\lambda}{\sinh \pi\lambda} \\ k(\beta) &= -\frac{1}{2i} \int d\lambda e^{-i\lambda\beta} \frac{\sinh(\pi - 2\nu)\lambda \cosh \nu\lambda}{\sinh \pi\lambda} \left[\frac{1}{\lambda + i\epsilon} + \frac{1}{\lambda - i\epsilon} \right] \\ k(\beta) + \int d\alpha J(\alpha - \beta) k(\alpha) &= -\frac{1}{2i} \int d\lambda e^{-i\lambda\beta} \frac{\cosh \nu\lambda}{2 \cosh 2\nu\lambda} \left[\frac{1}{\lambda + i\epsilon} + \frac{1}{\lambda - i\epsilon} \right] \\ &\rightarrow \pm \frac{\pi}{2}, \quad \text{for } \beta \rightarrow \pm\infty. \end{aligned} \quad (29)$$

Note that the $i\epsilon$ prescription is chosen so that $k(\pm\infty) = \pm(\pi - 2\nu)$, as required by the mapping. Finally, since $P_0 = 0$, we have for large α_+, α_- ,

$$\frac{P}{M} \approx -\frac{\pi}{2} \left[\int_{\alpha_+}^{\infty} - \int_{-\infty}^{\alpha_-} \right] \frac{d\beta}{2\pi} R(\beta). \quad (30)$$

Finally, we manipulate the expression for the energy, proportional to $-\ln T$, expressing it as an integral outside the interval (α_-, α_+) :

$$\begin{aligned} \frac{\ln T}{M} &= \int_{\alpha_-}^{\alpha_+} \frac{d\beta}{2\pi} R(\beta) \ln \left[\frac{\cosh \beta - \cos 3\nu}{\cosh \beta - \cos \nu} \right] \\ &= \int_{-\infty}^{\infty} \frac{d\beta}{2\pi} R(\beta) \ln \left[\frac{\cosh \beta - \cos 3\nu}{\cosh \beta - \cos \nu} \right] - \left[\int_{-\infty}^{\alpha_-} + \int_{\alpha_+}^{\infty} \right] \frac{d\beta}{2\pi} R(\beta) \ln \left[\frac{\cosh \beta - \cos 3\nu}{\cosh \beta - \cos \nu} \right] \\ &= \frac{\ln T_0}{M} - \left[\int_{-\infty}^{\alpha_-} + \int_{\alpha_+}^{\infty} \right] \frac{d\beta}{2\pi} R(\beta) \left(\ln t(\beta) + \int_{-\infty}^{\infty} d\alpha J(\alpha - \beta) \ln t(\alpha) \right), \end{aligned} \quad (31)$$

where we have written $t(\alpha)$ as shorthand for $t(k(\alpha))$. We use the Fourier transform of $\ln t(\alpha)$, given by

$$\ln t(\alpha) = \ln \left[\frac{\cosh \alpha - \cos 3\nu}{\cosh \alpha - \cos \nu} \right] = 2 \int d\lambda e^{-i\lambda\alpha} \frac{\sinh(\pi - 2\nu)\lambda \sinh \nu\lambda}{\lambda \sinh \pi\lambda}, \quad (32)$$

to arrive finally at a convenient expression for $E - E_0$ (Recall that $T = e^{-2aE}$, since the transfer matrix evolves two discrete time steps.):

$$\begin{aligned} \frac{E - E_0}{M} &= -\frac{\ln T - \ln T_0}{2aM} \\ &= \frac{1}{2a} \left[\int_{-\infty}^{\alpha_-} + \int_{\alpha_+}^{\infty} \right] \frac{d\beta}{2\pi} R(\beta) \int_{-\infty}^{\infty} d\lambda e^{-i\lambda\beta} \frac{\sinh \nu\lambda}{\lambda \cosh 2\nu\lambda} \\ &\approx \frac{1}{2a} \left[\int_{-\infty}^{\alpha_-} + \int_{\alpha_+}^{\infty} \right] \frac{d\beta}{2\pi} R(\beta) \frac{\sqrt{2}}{\cosh(\pi\beta/2\mu)}, \end{aligned} \quad (33)$$

where the last line is approximate, assuming large α_+, α_- . It is arrived at by first evaluating

$$\begin{aligned} \frac{\partial}{\partial \beta} \int_{-\infty}^{\infty} d\lambda e^{-i\lambda\beta} \frac{\sinh \nu\lambda}{\lambda \cosh 2\nu\lambda} &= -i \int_{-\infty}^{\infty} d\lambda e^{-i\lambda\beta} \frac{\sinh \nu\lambda}{\cosh 2\nu\lambda} \\ &= -\frac{\pi\sqrt{2} \sinh \pi\beta/2\mu}{\mu \cosh \pi\beta/2\mu} \\ &\rightarrow \begin{cases} -\pi\sqrt{2}e^{-\pi\beta/2\mu}/\mu & \text{for } \beta \rightarrow +\infty \\ +\pi\sqrt{2}e^{\pi\beta/2\mu}/\mu & \text{for } \beta \rightarrow -\infty \end{cases}, \end{aligned} \quad (34)$$

and then integrating the asymptotic form to get

$$\begin{aligned} \int_{-\infty}^{\infty} d\lambda e^{-i\lambda\beta} \frac{\sinh \nu\lambda}{\lambda \cosh 2\nu\lambda} &\rightarrow \begin{cases} 2\sqrt{2}e^{-\pi\beta/2\mu} & \text{for } \beta \rightarrow +\infty \\ 2\sqrt{2}e^{\pi\beta/2\mu} & \text{for } \beta \rightarrow -\infty \end{cases} \\ &\approx \frac{\sqrt{2}}{\cosh(\pi\beta/2\mu)}. \end{aligned} \quad (35)$$

To find the energy levels close to the ground state, we must analyze the equations for R for large α_+, α_- . For $\alpha > \alpha_+$ Eq. 21 can be approximated by dropping the integral over negative α and using the asymptotic form for R_0 :

$$R(\alpha) + \int_{\alpha_+}^{\infty} J(\alpha - \beta)R(\beta) \approx \frac{\pi}{\mu\sqrt{2}}e^{-\pi\alpha/2\mu}. \quad (36)$$

It is convenient to put

$$R(\alpha + \alpha^+) = \frac{\pi}{\mu\sqrt{2}}e^{-\pi\alpha_+/2\mu}S(\alpha)$$

so that Eq. 36 reduces to the Wiener-Hopf equation [3]

$$S(\alpha) + \int_0^{\infty} J(\alpha - \beta)S(\beta) = e^{-\pi\alpha/2\mu}. \quad (37)$$

Similarly, analyzing the equation for $\alpha < \alpha_-$, leads to the identification

$$R(\alpha + \alpha^-) \approx \frac{\pi}{\mu\sqrt{2}}e^{\pi\alpha_-/2\mu}S(-\alpha).$$

Inserting these approximations into the formulas for Q , P , and E , leads to

$$\begin{aligned} \frac{Q}{M} &\approx \frac{\pi}{\pi - \mu} \frac{1}{2\mu\sqrt{2}} \left[e^{-\pi\alpha_+/2\mu} + e^{\pi\alpha_-/2\mu} \right] \int_0^{\infty} d\beta S(\beta) \\ \frac{P}{M} &\approx -\frac{\pi}{2} \frac{1}{2\mu\sqrt{2}} \left[e^{-\pi\alpha_+/2\mu} - e^{\pi\alpha_-/2\mu} \right] \int_0^{\infty} d\beta S(\beta) \\ \frac{E - E_0}{M} &\approx \frac{1}{2a\mu} \left[e^{-\pi\alpha_+/\mu} + e^{\pi\alpha_-/\mu} \right] \int_0^{\infty} d\beta S(\beta) e^{-\pi\beta/2\mu}. \end{aligned} \quad (38)$$

Next one can solve the first two equations for α_+ and α_- and substitute in the last equation to get

$$\frac{E - E_0}{M} \approx \frac{4\mu}{2a} \frac{I(\pi/2\mu)}{I(0)^2} \left[\frac{(\pi - \mu)^2}{\pi^2} \frac{Q^2}{M^2} + \frac{4}{\pi^2} \frac{P^2}{M^2} \right], \quad (39)$$

where we have defined $I(x) = \int_0^{\infty} d\beta S(\beta)e^{-x\beta}$. From the solution of Eq. 37 one can infer (see [3]) that $I(\pi/2\mu)/I(0)^2 = \pi^2/8\mu(\pi - \mu)$, so finally

$$E - E_0 \approx \frac{1}{aM} \left[\frac{\pi - \mu}{4} Q^2 + \frac{1}{\pi - \mu} P^2 \right] = \frac{T_0}{P^+} \left[\frac{\pi - \mu}{4} Q^2 + \frac{1}{\pi - \mu} P^2 \right], \quad (40)$$

regaining a key result of [1].

4.2 Non-consecutive I_l

The excited states included in Eq. 40 are those where the numbers I_l are consecutive. For example, the state with $Q = P = 0$ corresponds to the choice (with $q = M/2$ odd)

$$\left(-\frac{q-1}{2}, \dots, \frac{q-3}{2}, \frac{q-1}{2} \right).$$

There are also excitations in which ‘‘holes’’ are allowed in this set of numbers. As an example, consider replacing $(q-1-2j)/2$ in the above list by $(q+1)/2$, creating a gap, but retaining the

same number of overturned arrows, so that $Q = 0$. However the momentum is increased by the amount $P = 2\pi(j+1)/M$. For large M , the effect of this hole on the k 's is small, and it makes sense to expand them around the values appropriate to the $Q = P = 0$ state, the new set of k 's differing from the latter by δk_j . Referring to the original equation for the k 's, we find an equation for δk :

$$\begin{aligned}\delta k_l &= \frac{2\pi}{M}\theta(l-l_j) + \frac{2\pi}{M}\sum_{j \neq l} \left[-\frac{\partial \alpha_j}{\partial k_j} \delta k_j + \frac{\partial \alpha_l}{\partial k_l} \delta k_l \right] K(\alpha_l - \alpha_j) \\ \delta k_l \left(1 - \frac{\partial \alpha_l}{\partial k_l} \frac{2\pi}{M} \sum_{j \neq l} K(\alpha_l - \alpha_j) \right) &= \frac{2\pi}{M}\theta(l-l_j) - \frac{2\pi}{M}\sum_{j \neq l} \left[\frac{\partial \alpha_j}{\partial k_j} \delta k_l \right] K(\alpha_l - \alpha_j) \\ \delta k(\alpha) \frac{\partial \alpha}{\partial k} R(\alpha) &= \frac{2\pi}{M}\theta(\alpha - \alpha_j) - \int d\beta \frac{\partial \beta}{\partial k} \delta k(\beta) R(\beta) K(\alpha - \beta),\end{aligned}\quad (41)$$

where we have replaced the sums by integrals in the last line. Defining $\chi(\alpha) = M\delta k(\alpha)R(\alpha)d\alpha/dk$, we have the integral equation

$$\chi(\alpha) + \int_{-\infty}^{\infty} d\beta K(\alpha - \beta)\chi(\beta) = 2\pi\theta(\alpha - \alpha_j).\quad (42)$$

Here α_j marks the location of the ‘‘hole’’. It can be related to the value for the momentum of the excited state:

$$P = \frac{2\pi(j+1)}{M} = \sum_l \delta k_l = \int_{-\infty}^{\infty} \frac{d\alpha}{2\pi} \chi(\alpha) \frac{dk}{d\alpha}\quad (43)$$

Similarly, we can write the energy difference between the excited and ground state as

$$\begin{aligned}E - E_0 &= \frac{1}{2a}(\ln T_0 - \ln T) = -\frac{1}{2a} \sum_l \delta k_l \frac{d\alpha_l}{dk_l} \frac{1}{t_l} \frac{dt_l}{d\alpha_l} \\ &= -\frac{1}{2a} \int_{-\infty}^{\infty} \frac{d\alpha}{2\pi} \chi(\alpha) \left[\frac{\sinh \alpha}{\cosh \alpha - \cos 3\nu} - \frac{\sinh \alpha}{\cosh \alpha - \cos \nu} \right]\end{aligned}\quad (44)$$

Eq. 42 can be immediately solved via Fourier transformation:

$$\chi(\alpha) = i \int d\lambda e^{-i(\alpha - \alpha_j)\lambda} \frac{\sinh \pi \lambda}{2(\lambda + i\epsilon) \sinh(\pi - \mu)\lambda \cosh \mu \lambda},\quad (45)$$

and used to obtain the total momentum and energy

$$\begin{aligned}P &= \frac{i}{2} \int d\lambda e^{-i\lambda\alpha_j} \frac{\cosh \nu \lambda}{(-\lambda + i\epsilon) \cosh 2\nu \lambda} \\ E - E_0 &= -\frac{1}{2a} \int d\lambda e^{-i\lambda\alpha_j} \frac{\sinh \nu \lambda}{(-\lambda + i\epsilon) \cosh 2\nu \lambda}.\end{aligned}\quad (46)$$

Of course, we are interested in these expressions in the limit $\alpha_j \rightarrow \infty$, corresponding to the continuum limit. This asymptotic limit is obtained by deforming the integration contours into the lower half plane and picking up the nearest pole to the real axis, namely the one at $\lambda = -i\pi/4\nu$. This leads to

$$P \sim \sqrt{2}e^{-\pi\alpha_j/4\nu} \quad E - E_0 \sim \frac{\sqrt{2}}{a}e^{-\pi\alpha_j/4\nu},\quad (47)$$

from which we conclude that

$$E - E_0 = \frac{P}{a} = \frac{2\pi(j+1)}{Ma} = \frac{2\pi(j+1)T_0}{P^+} \quad (48)$$

in the limit $M \rightarrow \infty$. Notice the important fact that the energy of these excitations is independent of the vertex weight v . Although we have discussed only one particular “particle-hole” excitation, it is clear that the energy of the state with many particle-hole pairs will simply be additive in the momentum carried by each pair. Furthermore, there are two independent sets of such excitations about the two boundaries of the Fermi sea. Each particle hole excitation contributes $2\pi n T_0 / P^+$, where $n > 0$. If there are several particle-hole pairs from the right side $k > 0$ of the Fermi sea, we define $N_R = \sum_i n_i$, and similarly N_L is defined for those from the left side $k < 0$ of the Fermi sea.

These contributions to the energy are added to those arising from non-zero Q, P . Note that the P^2 term in the energy receives negligible contributions from particle-hole excitations from the same side of the Fermi sea, since these have $P = O(1/M)$. This term is non-zero in the continuum limit only if the particle and hole are from opposite sides of the sea. For example, replacing $-(q+1)/2$ with $(q+1)/2$ contributes $2\pi q/M \approx \pi$ to P . But such large momentum pair excitations have already been accounted for among the excitations with consecutive I_l considered earlier. Thus the energy levels of the continuum limit are determined by Q, P, N_R , and N_L :

$$E - E_0 = \frac{T_0}{2P^+} \left[\frac{\pi - \mu}{2} Q^2 + \frac{2}{\pi - \mu} P^2 + 4\pi(N_R + N_L) \right]. \quad (49)$$

Recall that $Q = 2r$ and $P = \pi s$ where r, s range independently over all integers.

5 Discussion and Concluding Remarks

We conclude by recalling the comparison of the energy spectrum just obtained with that of a compactified scalar field on the continuum closed string world-sheet [1], described by the action

$$S = \frac{1}{2} \int d\tau \int_0^{P^+} d\sigma (\dot{\phi}^2 - T_0^2 \phi'^2) \quad (50)$$

with the equivalence relation

$$\phi \equiv \phi + 2\pi R. \quad (51)$$

We would like to identify ϕ/R with the angle of the $O(2)$ rotations of the underlying symmetry of the theory. It should therefore be conjugate to the charge Q . Thus we take Q proportional to the zero mode of the conjugate momentum to ϕ ,

$$\int_0^{P^+} d\sigma \dot{\phi} = \frac{k}{R} = \frac{Q}{2R}. \quad (52)$$

Then P must be taken proportional to the winding number l defined by the boundary condition $\phi(P^+) = \phi(0) + 2\pi l R$. The energy of the compactified scalar field is therefore

$$E = \frac{1}{2P^+} \left[\frac{k^2}{R^2} + 4\pi^2 l^2 T_0^2 R^2 + 4\pi T_0 (N_R + N_L) \right], \quad (53)$$

from which we infer that $R^2 = 1/(2T_0(\pi - \mu))$. Remembering that $\cos \mu = \cos 2\nu = \text{Re } e^{2i\nu} = -1 + 1/2v^2$, we see that the radius of the circle on which the field lives is determined by the ratio

of quartic couplings. In particular the limit $R \rightarrow \infty$ implies $\mu \rightarrow \pi$ or $v \rightarrow \infty$. The self dual radius $R_*^2 = 1/2\pi T_0$ corresponds to $\mu = 0$ or $v = 1/2$. Thus the range of couplings considered here $1/2 \leq v < \infty$ (for which the 6-vertex model is critical) produces circle radii $R_* \leq R < \infty$. Interestingly, small radii, $R < R_*$ are not accessible in the vertex model. For $v < 1/2$ the model is not critical and the continuum limit accordingly sends all excitations to infinite energy, i.e. there is no interesting continuum limit.

The important message of [1] is that if string can be understood as a composite of field quanta along the lines of the fishnet model, then internal degrees of freedom carried by the fields are naturally promoted to world-sheet fields. Among the possible interpretations of these world-sheet fields is that they represent extra compact dimensions. The simple $O(2)$ model reviewed in this article leads to the emergence of an extra circular dimension S_1 . Within the fishnet model, it will certainly be interesting to study the $SO(n)$ case. If the $n = 2$ case is a fair guide, we can hope that what will emerge is a world-sheet field that lives on the sphere S_{n-1} . This would be the $SO(n)$ nonlinear sigma model. The vertex model in this case is much more complicated than the 6-vertex model: each line of the diagram can be in n states, and there are many more distinct vertices. For instance, in the $n = 3$ case there are 19 vertices that conserve the 3-component of spin. These models are currently under study.

The fishnet model is at best relevant only to the strong coupling behavior of the underlying quantum field theory. Even then we do not yet fully understand how fishnets fit in to the most well-established string/field duality, $AdS_5 \times S_5 / \mathcal{N} = 4$ SUSY Yang-Mills. Optimistically, the mechanism illustrated in this paper will shed light on the field theoretic origin of the S_5 part of the ten dimensional space-time manifold: the Yang-Mills super-multiplet contains 6 scalar fields that transform under the vector representation of $SO(6)$. The conjecture of the previous paragraph suggests that fishnets propagating only these scalars would describe the $SO(6)$ nonlinear sigma model, leading to the emergence of S_5 .

But in its simplest presentation, the dense fishnet model produces flat Minkowski space-time for the remaining non-compact dimensions, not anti-de Sitter space-time. We believe that this flaw is present because the dense fishnets completely freeze out both fluctuations in the number of field quanta *and* fluctuations in the distribution of P^+ along string. Properly including the gauge fields in the fishnet approach could improve this situation by allowing some of these fluctuations even at strong coupling [8]. Indeed, since the $SO(n)$ nonlinear sigma model is not conformally invariant for $n > 2$, consistency of the string interpretation requires a nontrivial dynamical interplay between the S_5 degrees of freedom and the space-time degrees of freedom in the world-sheet action. As presently understood, the AdS/CFT connection [2] implements this via the AdS metric and the 5-form Ramond-Ramond flux on S_5 . More concretely, the light-cone treatment of string on $AdS_5 \times S_5$ [12, 13] indicates how these interactions appear in the world-sheet action, in which the 5th dimension plays a role similar to the Liouville field in restoring conformal invariance. It remains to be seen whether the graph summation approach can adequately account for these features.

Acknowledgments: I wish to thank Arkady Tseytlin for many stimulating discussions and Achim Kempf for critically reading the manuscript. This work is supported in part by U.S. DOE grant DE-FG02-97ER-41029.

References

- [1] R. Giles, L. McLerran, and C. B. Thorn, *Phys. Rev.* **D17** (1978) 2058.
- [2] J. M. Maldacena, *Adv. Theor. Math. Phys.* **2** (1998) 231-252, hep-th/9711200.

- [3] C. N. Yang and C. P. Yang, *Phys. Rev.* **150** (1966) 321; *Phys. Rev.* **150** (1966) 327.
- [4] E. H. Lieb, *Phys. Rev. Lett.* **18** (1967) 692; *Phys. Rev.* **162** (1967) 162.
- [5] E. H. Lieb, *Phys. Rev. Lett.* **18** (1967) 1046; B. McCoy and T. T. Wu, *Nuovo Cimento* **56B** (1968) 311; B. Sutherland, *J. Math. Phys.* **11** (1970) 3183.
- [6] H. B. Nielsen and P. Olesen, *Phys. Lett.* **32B** (1970) 203; B. Sakita and M. A. Virasoro, *Phys. Rev. Lett.* **24** (1970) 1146.
- [7] C. B. Thorn, *Phys. Lett.* **70B** (1977) 85; *Phys. Rev.* **D17** (1978) 1073.
- [8] K. Bering, J. S. Rozowsky and C. B. Thorn, *Phys. Rev.* **D61** (2000) 045007, hep-th/9909141.
- [9] R. Giles and C. B. Thorn, *Phys. Rev.* **D16** (1977) 366.
- [10] P. Goddard, J. Goldstone, C. Rebbi, and C. B. Thorn, *Nucl. Phys.* **B56** (1973) 109.
- [11] H. A. Bethe, *Z. Phys.* **61** (1930) 206.
- [12] R. R. Metsaev and A. A. Tseytlin, Superstring action in AdS(5) x S**5: kappa-symmetry light cone gauge, hep-th/0007036.
- [13] R. R. Metsaev, C. B. Thorn and A. A. Tseytlin, Light-cone superstring in AdS space-time, hep-th/0009171.